AIAA JOURNAL
Vol. 33, No. 12, December 1995

Technical Notes

TECHNICAL NOTES are short manuscripts describing new developments or important results of a preliminary nature. These Notes cannot exceed 6 manuscript pages and 3 figures; a page of text may be substituted for a figure and vice versa. After informal review by the editors, they may be published within a few months of the date of receipt. Style requirements are the same as for regular contributions (see inside back cover).

Vortex Characteristics over Delta Wing Subject to Transient Along-Core Blowing

Cheng-Hsiung Kuo* and Ni-Yu Lu†
National Chung-Hsing University,
40227 Taichung, Taiwan, Republic of China

Introduction

THIS investigation is primarily focused on the poststall vortical structure over delta wing with a 75-deg sweep angle and its transient characteristics in response to various kinds of blowing perturbation issuing from the apex of the delta wing and along the vortex core (Fig. 1a). Some important results on the time constant of the vortex breakdown recovery process and its dependence on the angle of attack and blowing rates, as well as the type of blowing, will be addressed.

Control of vortical structure over delta wings can be attained in many respects. Tavella[1] and Wood and Robert[2] found that direct control of the vorticity fed as a result of the separation from the leading edge exerts a significant influence on the vortical structure up to an angle of attack (AOA) of 60 deg. Moreover, Bradley et al.[3] and Campbell[4] showed that spanwise blowing can also generate a large increase in lift at high AOA at Mach numbers 0.35 and 0.75 for a lower sweep angle. Shi et al.[5] and Visser et al.[6] demonstrated the importance of the location and orientation of blowing in determining the position of vortex breakdown. Recently, Parmenter and Rockwell[7] addressed the restabilization of the leading-edge vortex over the delta wing by transient suction at a location downstream of breakdown. The hysteresis of the vortex response and the time lag for restabilization of the vortex core are reported.

Studies of the dynamic behavior of the leading-edge vortices on a delta wing undergoing oscillatory motion reveal that breakdown location exhibits a hysteresis loop and is frequency dependent. A general transfer function of the vortex core condition and the external perturbation, however, still remain unclear. Therefore, the purpose of this investigation is to understand the transient behavior of the vortical structure over a delta wing subjected to along core blowing issued from the wing apex. The time constant of the vortex breakdown recovery process is found to depend strongly on the AOA and blowing rate, as well as the type of blowing. Furthermore, the vortex core in response to blowing along the vortex core is also frequency dependent and behaves like a low-pass filter.

Experimental Setup

The experiments were conducted in a low-speed water channel with cross section of 40 × 40 cm^2 and 250 cm in length. The flow conditions are controlled to reduce turbulence intensity down to a level of 0.46% at a Reynolds number of 2×10^4. The nonuniformity, based on the difference between the maximum and minimum of the freestream velocity distributions measured by laser Doppler anemometer (LDA), is around 1.2%. The blockage ratio of the half-wing model varies between 0.024 and 0.031 for different AOA. The momentum coefficient of blowing is defined as $C_\mu = (V_p/U_\infty)^2\,(A_p/A_w)$, where V_p and U_∞ are the velocities issuing from the blowing slot and in the freestream and A_p and A_w are the areas of the blowing slot and the half-wing model, respectively. In this study, the momentum coefficient varied in the range of 0.025–0.181, and the reduced frequencies vary between 1.25 and 5.0.

Figure 1a shows the direction and location where the blowing perturbation is applied. In Fig. 1b, the half-delta wing model, with 75-deg sweep and 25-deg upward-beveled leading edge, is situated on a platform having an elliptic leading edge profile with a major/minor axes ratio of 5:1. The model is located within the region where the static pressure indicates only a negligible streamwise pressure gradient in presence of the platform. A circular disk is designed to rotate relative to the wing model to align the blowing direction with the vortex core above the wing surface. A hole is drilled through the thickness of the circular disk to align with the vortex core direction when viewed from the wing upper surface. Fluid issues from this blowing slot, 0.5 mm inner diameter, into and along the vortex core driven by a stepping motor pumping system. The AOA can be altered simply by screwing each hole to the wing model with the wing tip as a rotating center. Food-coloring dye, flowing naturally from another tiny slot very close to the wing apex, has been used as a tracer in the vortex core to identify the transient location of vortex breakdown during and after each blowing event. The vortex breakdown is qualitatively characterized by the

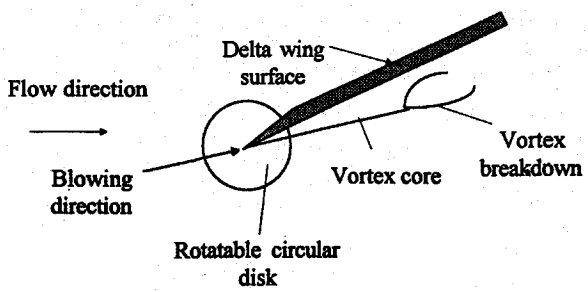

Fig. 1a Closeup of blowing location and orientation near the wing apex.

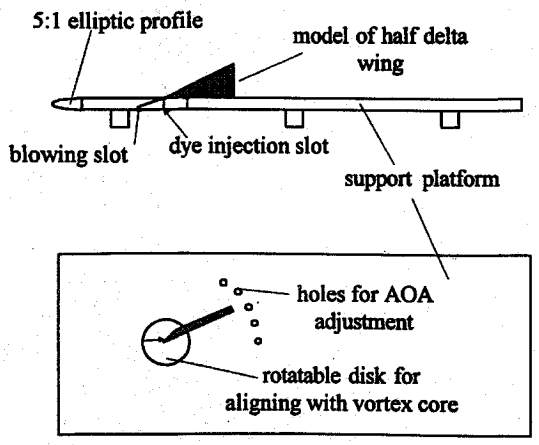

Fig. 1b Installation of half-delta wing model.

Received Nov. 26, 1994; revision received July 31, 1995; accepted for publication July 31, 1995.

*Associate Professor, Department of Mechanical Engineering.
†Graduate Student, Department of Mechanical Engineering.

appearance of an abrupt divergence of the core diameter. Moreover, a scale accurate to $\frac{1}{40}$ of the root chord is used for more precise measurement using a video monitor. Blowing rate and duration are controlled through a personal computer-based control module by programming different numbers of output pulses to the stepping motor driver. Furthermore, with proper installation of two one-way valves, the blowing can be performed as a single, a periodic, or a continuous event.

Results and Discussions

Single Blowing

Here, single blowing means that the blowing is maintained at constant rate for a period of $T^* = TU_\infty/C = 0.4$. The normalized maximum distance X_b/C of the vortex breakdown over the stationary half-delta wing after the cessation of blowing at various blowing rates and for different AOA is shown in Fig. 2. The vortex breakdown location at zero blowing rate represents a long time-averaged unperturbed position that varies for different AOA. As can be seen, vortex breakdown is further delayed whenever blowing is applied through the wing apex and along the vortex core. Since blowing rate is defined as the rate of change of linear momentum, a higher blowing rate represents larger external force input into and along the vortex core. The large external force input can overcome the adverse pressure gradient along the vortex core, near the vortex breakdown region, and hence substantially delay the vortex breakdown. Moreover, it is evident that the slopes in Fig. 2 for $\alpha = 45$ and 40 deg are larger than that for $\alpha = 35$ deg when $C_\mu \leq 0.10$. Simply, the flow physics are that the vortex core is shorter and the vortex breakdown position is closer to the apex of the wing at higher AOA. Therefore, the momentum addition per unit time (force) issuing from the apex can be efficiently transferred to the vortex core to overcome the adverse pressure gradient along the vortex core, especially near the breakdown region. From a practical point of view, $C_\mu \leq 0.10$ might be a good threshold of blowing rate at which the delay of vortex breakdown is much more sensitive at higher AOA within the poststall regime when undergoing a single blowing perturbation.

Periodic Blowing

In these experiments, periodic blowing is controlled by the same mechanism, and the reduced frequencies $f_r = fC/U_\infty$ are between 1.25 and 5.0, as shown in Fig. 3. The periodic blowing is also applied to and along the vortex core for several cycles and stops at the moment when vortex breakdown shows little movement. All of the recovery time sequences are recorded from this steady position to minimize the error due to the unsteady nature of vortex breakdown. The dependence of maximum vortex core length prior to breakdown on the reduced frequency is shown in Fig. 3. The vortex breakdown can be effectively delayed, especially at low reduced frequency. This implies that the response of the vortex core to adjust itself to the environmental change is a slowly varying process. The maximum vortex core length decreases monotonically as the reduced frequency gets higher. At higher reduced frequencies, the vortex core does not have enough time to adjust to the perturbation, and hence can get only little benefit from the supplied momentum.

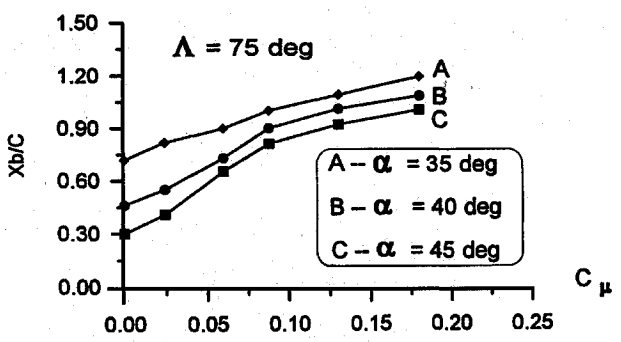

Fig. 2 Maximum vortex core length in relation to blowing coefficient at various AOA subject to a single blowing.

Table 1 Dimensionless time constant of vortex breakdown recovering from the instant of blowing cessation

	Single blowing, $\tau^* = \tau U_\infty/C$		
AOA, deg	$C_\mu = 0.088$	$C_\mu = 0.131$	$C_\mu = 0.181$
$\alpha = 40$	1.932	2.20	2.6
$\alpha = 45$	1.884	2.12	2.52

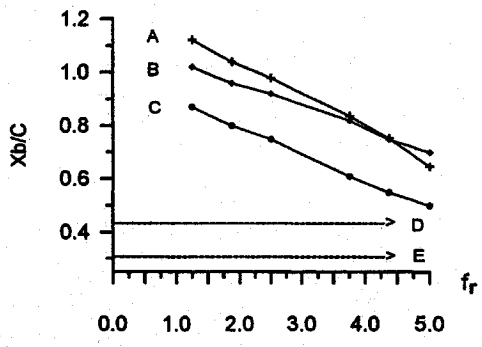

Fig. 3 Farthest location of vortex breakdown as function of reduced frequency: *D*—$C_\mu = 0.00$, $\alpha = 40$ deg; *E*—$C_\mu = 0.00$, $\alpha = 45$ deg; *A*—$C_\mu = 0.06$, $\alpha = 40$ deg; *B*—$C_\mu = 0.088$, $\alpha = 45$ deg; *C*—$C_\mu = 0.06$, $\alpha = 45$ deg.

Moreover, as seen in Fig. 3, the delay of vortex breakdown is also dependent on the blowing rate and the AOA. When blowing at fixed f_r for $\alpha = 45$ deg, the higher the blowing rate is, the further the delay of the vortex breakdown location. Careful examinations of the data reveals that for fixed AOA the delay for higher blowing rate at higher reduced frequency is not so efficient as that for a lower blowing rate applied at lower reduced frequency. This result also suggests the practical importance of small blowing rates in combination with small reduced frequency to control the vortex structure over a delta wing. In addition, the delay, when perturbed at the same blowing rate, is more effective for $\alpha = 40$ deg than for $\alpha = 45$ deg. Furthermore, the output/input ratio, in terms of $(X_b - X_i)/X_i$, tends to be zero (i.e., approaches to the level of unperturbed core length X_i as can be seen by the dash lines D or E in Fig. 3 for different AOA) at higher reduced frequency; however, it leads to finite value at lower reduced frequency. This fact implies that the vortex core behaves like a low-pass filter when perturbed periodically along the vortex core.

Characteristic Time Scale

The transient time sequences of vortex breakdown recovery all exhibit a monotonic upstream motion toward the unperturbed location without any discernible oscillatory behavior. Therefore, the time constant τ is an important characteristic governing the vortex breakdown recovery process. This characteristic time scale determines the response of the vortex core to various kinds of blowing perturbation and will provide a guide of control of the vortex core over a delta wing, especially within the poststall AOA range. Within the trailing edge, the monotonic decrease of the transient behavior of vortex breakdown after cessation of blowing has similar characteristics to the exponential decay solution. With condition at large time, corresponding to an unperturbed core length, and at cessation of blowing, corresponding to the maximum vortex core length, the characteristic time constants of these transient time sequences can be found by fitting all data points onto each exponential decay curve. The results are listed in Table 1 for the single blowing perturbation. It is evident that the dimensionless time constant $\tau^* = \tau U_\infty/C$ decreases as AOA increases. This implies that at higher AOA there exists a stronger adverse pressure gradient along the vortex core and near the breakdown region; thus vortex breakdown has stronger tendency to recover to its unperturbed position. For fixed AOA, however, the characteristic time constant gets larger as the blowing rate increases. For cases under periodic blowing, listed in Table 2 for different AOA and blowing rate, it is evident that the time constant at small reduced frequency is much larger than those at large reduced frequency. Moreover, the effect of AOA on τ^* is substantially enhanced at low reduced frequency.

Table 2 Dimensionless time constant of vortex breakdown recovering from the instant of blowing cessation

AOA, deg		Periodic blowing, $\tau^* = \tau U_\infty / C$			
		$f_r = 1.25$	$f_r = 2.5$	$f_r = 3.75$	$f_r = 5.0$
$\alpha = 45$	$C_\mu = 0.06$	2.52	1.86	1.28	0.84
$\alpha = 45$	$C_\mu = 0.088$	3.04	2.56	2.16	1.68
$\alpha = 40$	$C_\mu = 0.06$	3.2	2.44	1.72	0.96

Acknowledgment

The authors are grateful for the support of this investigation from the National Science Foundation of Republic of China under Grant NSC-82-0618-E-005-096.

References

[1]Tavella, D., "Lift of Delta Wings with Leading Edge Blowing," *Journal of Aircraft*, Vol. 25, No. 6, 1987, pp. 522–524.

[2]Wood, N. J., and Robert, L., "Control of Vortical Lift on Delta Wings by Tangential Leading Edge Blowing," *Journal of Aircraft*, Vol. 25, No. 3, 1987, pp. 236–243.

[3]Bradley, R. G., Whitten, P. D., and Wray, W. O., "Leading-Edge Vortex Augmentation in Compressible Flow," *Journal of Aircraft*, Vol. 13, No. 9, 1976, pp. 238–242.

[4]Campbell, J. F., "Augmentation of Vortex Lift by Spanwise Blowing," *Journal of Aircraft*, Vol. 13, No. 9, 1976, pp. 727–732.

[5]Shi, Z., Wu, J. M., and Vakili, A. D., "An Investigation of Leading-Edge Vortices on Delta Wing With Jet Blowing," AIAA Paper 87-0330, Jan. 1987.

[6]Visser, K. D., Iwanski, K. T., Nelson, R. C., and Ng, T. T., "Control of Leading-Edge Vortex Breakdown By Blowing," AIAA Paper 88-0504, Jan. 1988.

[7]Parmenter, K., and Rockwell, D., "Transient Response of Leading Edge Vortices to Localized Suction," *AIAA Journal*, Vol. 28, No. 6, 1990, pp. 1131–1133.

Conjugate Gradient Squared Algorithm for Panel Methods

Santhosh P. Koruthu*
Aeronautical Development Agency, Bangalore 560 017, India

Introduction

PANEL methods are the most efficient of numerical schemes to obtain solutions to linear potential flow problems. The efficiency of these methods arises primarily from the fact that, in a panel method, the effective dimensionality of the problem is one less than the spatial dimension of the flowfield. This is because the problem of solving the governing partial differential equation for the field is transformed into an equivalent problem of solving an integral equation for the surface. Panel methods solve this integral equation numerically. The efficiency of these methods makes them useful tools in tradeoff studies in aircraft design.

Numerical solution of the integral equation using a panel method gives rise to fully populated linear systems, in general. This is in contrast with the finite difference, finite element, and finite volume techniques employed in computational fluid dynamics where each linearized step in the solution algorithm gives rise to a sparse linear system. When the flow past a complicated configuration is analyzed using a panel method, it is difficult to ensure any specific structure to the matrix of the linear system. Often, diagonal dominance cannot be assured. Therefore, when solving such systems, most classical iterative schemes are slow in convergence. Many panel codes use Gaussian elimination [lower-upper (LU) decomposition] as an alternative.[1] This requires $\mathcal{O}(n^3)$ floating point operations where n is the order of the matrix. An iterative scheme requires only $\mathcal{O}(n^2)$ floating point operations. Therefore it is desirable to have robust iterative schemes, especially for situations where the order of the matrix is large, such as would be the case when analyzing flow past complex configurations.

A variety of conjugate gradient type methods have evolved as potential linear system solvers. The conjugate gradient squared (CGS) method is one that has been proposed for nonsymmetric and nonpositive definite systems.[2] The present paper examines the use of this scheme for systems of linear algebraic equations encountered in panel methods.

Present Panel Method

A low-order panel method for subcritical flows has been used in the present study. The governing flow equation is the Prandtl–Glauert equation for the velocity potential ϕ:

$$(1 - M_\infty^2)\phi_{xx} + \phi_{yy} + \phi_{zz} = 0 \tag{1}$$

Here subscripts denote partial differentiation; M_∞ is the freestream Mach number. Using a stretching transformation, this equation is reduced to the Laplace equation:

$$\phi_{xx} + \phi_{yy} + \phi_{zz} = 0 \tag{2}$$

The Laplace equation is transformed into an integral equation using Green's theorem. For a point P,

$$4\pi\phi(P) = \int_S [\phi] G_1 \, dS + \int_S [\text{grad}\,\phi \cdot \hat{n}] G_2 \, dS + 4\pi\phi_\infty \tag{3}$$

The brackets [ ] refer to a jump in the enclosed quantity across the boundary S; $\hat{n}$ is the unit normal to surface S; ϕ_∞ is the freestream potential. It may be noted that G_1 is Green's function for a doublet and G_2 is Green's function for a source. The corresponding jump quantities in Eq. (3) can therefore be considered as doublet and source strengths. These are the unknown quantities to be determined in a panel method that solves Eq. (3) numerically.

In the present method, the source strength is prescribed a priori as the negative of the component of the freestream velocity vector normal to the surface. A Dirichlet boundary condition on the internal perturbation potential is applied to obtain the unknown doublet strength. To numerically evaluate the integrals in Eq. (3), the surface of the configuration is divided into n flat panels. The centroid of each panel is chosen as the panel control point, where boundary conditions are applied. The influence (in terms of the induced velocity potential) on the control point on each panel i, of unit constant strength singularity distribution on each panel j, is calculated. For the source distributions, this influence is denoted by B_{ij}. For the doublet distributions, the influence is A_{ij}. Application of the boundary condition (of zero internal perturbation potential) at a control point i, using Eq. (3), gives rise to the equation

$$\sum_j A_{ij}\mu_j + \sum_j B_{ij}\sigma_j = 0 \tag{4}$$

where σ_j and μ_j are, respectively, the source strength and the doublet strength on the jth panel. Since the source strengths σ_j are prescribed, writing down Eq. (4) for each panel i gives rise to a linear system

$$Ax = b \tag{5}$$

The solution of this system determines the unknown doublet strengths that uniquely determine the flowfield. Further details of the present method may be found in Ref. 3.

CGS Algorithm and Present Implementation

Conjugate gradient (CG) algorithms are known to be very efficient for solving symmetric, positive definite linear systems. The

Received July 20, 1994; revision received Feb. 27, 1995; accepted for publication Feb. 28, 1995.

*Project Manager, P.B. No. 1718, Vimanapura Post.